

Energy levels and transition data of $3p^6 3d^8$ and $3p^5 3d^9$ configurations in Fe-like ions (Z = 57, 60, 62, 64, 65)

Bao-Ling Shi(施宝玲), Yi Qin(秦毅), Xiang-Fu Li(李向富), Bang-Lin Deng(邓邦林), Gang Jiang(蒋刚), and Xi-Long Dou(豆喜龙)

Citation: Chin. Phys. B, 2022, 31 (**5**): 053102. DOI: 10.1088/1674-1056/ac4480
Journal homepage: http://cpb.iphy.ac.cn; http://iopscience.iop.org/cpb

What follows is a list of articles you may be interested in

Spectroscopy and scattering matrices with nitrogen atom: Rydberg states and optical oscillator strengths

Yuhao Zhu(朱宇豪), Rui Jin(金锐), Yong Wu(吴勇), and Jianguo Wang(王建国)
Chin. Phys. B, 2022, 31 (**4**): 043103. DOI: 10.1088/1674-1056/ac1f05

Transition parameters of Li-like ions (Z=7-11) in dense plasmas

Xiang-Fu Li(李向富), Li-Ping Jia(贾利平), Hong-Bin Wang(王宏斌), and Gang Jiang(蒋刚)
Chin. Phys. B, 2021, 30 (**5**): 053102. DOI: 10.1088/1674-1056/abea80

Analytical expressions of non-relativistic static multipole polarizabilities for hydrogen-like ions

Xuesong Mei(梅雪松), Wanping Zhou(周挽平), Zhenxiang Zhong(钟振祥), Haoxue Qiao(乔豪学)
Chin. Phys. B, 2020, 29 (**4**): 043101. DOI: 10.1088/1674-1056/ab75d0

Vibronic spectra of aluminium monochloride relevant to circumstellar molecule

Jian-Gang Xu(徐建刚), Cong-Ying Zhang(张聪颖), Yun-Guang Zhang(张云光)
Chin. Phys. B, 2020, 29 (**3**): 033102. DOI: 10.1088/1674-1056/ab6c46

Study of highly excited vibrational dynamics of HCP integrable system with dynamic potential methods

Aixing Wang(王爱星), Lifeng Sun(孙立风), Chao Fang(房超), Yibao Liu(刘义保)
Chin. Phys. B, 2020, 29 (**1**): 013101. DOI: 10.1088/1674-1056/ab593a

---

Energy levels and transition data of $3p^63d^8$ and $3p^53d^9$ configurations in Fe-like ions ($Z = 57, 60, 62, 64, 65$)

Bao-Ling Shi(施宝玲)[1,†], Yi Qin(秦毅)[1,†], Xiang-Fu Li(李向富)[2], Bang-Lin Deng(邓邦林)[3], Gang Jiang(蒋刚)[1,‡], and Xi-Long Dou(豆喜龙)[1]

[1] *Institute of Atomic and Molecular Physics, Sichuan University, Chengdu* 610065, *China*
[2] *College of Electrical Engineering, Longdong University, Qingyang* 745000, *China*
[3] *College of Geophysics, Chengdu University of Technology, Chengdu* 610059, *China*

(Received 13 November 2021; revised manuscript received 14 December 2021; accepted manuscript online 18 December 2021)

Atomic data of highly charged ions (HCIs) offer an attractive means for plasma diagnostic and stars identification, and the investigations on atomic data are highly desirable. Herein, based on the fully relativistic multi-configuration Dirac–Hartree–Fock (MCDHF) method, we have performed calculations of the fine-structure energy levels, wavelengths, transition rates, oscillator strengths, and line strengths for the lowest 21 states of $3p^63d^8$–$3p^53d^9$ electric dipole (E1) transitions configurations in Fe-like ions ($Z = 57$, 60, 62, 64, 65). The correlation effects of valence–valence (VV) and core–valence (CV) electrons were systematically considered. In addition, we have taken into account transverse-photon (Breit) interaction and quantum electrodynamics (QED) corrections to treat accurately the atomic state wave functions in the final relativistic configuration interaction (RCI) calculations. Our calculated energy levels and transition wavelengths are in excellent agreement with the available experimental and theoretical results. Most importantly, we predicted some new transition parameters that have not yet been reported. These data would further provide critical insights into better analyzing the physical processes of various astrophysical plasmas.

Keywords: Fe-like ions, energy levels, wavelengths, transition rates

PACS: 31.15.ag, 31.15.xr, 31.30.jc, 95.30.Ky **DOI:** 10.1088/1674-1056/ac4480

1. Introduction

Atomic structure parameters have been considered as a promising approach to improve our understanding of the physical processes of astrophysical plasmas.[1–4] On the other hand, knowledge of emission lines generated by these high-Z elements is essential for the abundance of stars.[5] It is therefore a continuous focus of attention. Considerable attempts, including laser-produced plasmas, grazing-incidence spectrographs, electron-beam ion trap (EBIT), tokamak plasmas, *etc.*, have been devoted to excavating these atomic data and won considerable achievements.[6–11] However, the current atomic data are still insufficient in explanation of the existing results.

Among these highly charged ions, of particular interest are Fe-like ions. Its wavelengths and transition rates are useful for studying the abundance of stars.[12,13] Experimentally the spectrum of Fe-like ions is primarily produced by laser-produced plasmas. Its emission lines, in general, range from x-ray to extreme ultraviolet (EUV) spectral regions.[14] These emission spectrums have profound implications not only for spectral diagnosis in inertial confinement fusion experiments, but also for analyzing the abundance of galaxy clusters and the geometry of star flares.[15] These applications stimulated extensive researches on atomic structure parameters for Fe-like ions. Ekberg *et al.*[16,17] investigated the landscape of energy levels and wavelengths of the $3p^63d^8$–$3p^53d^9$ E1 transitions configurations for Fe-like ions ($44 \leq Z \leq 70$) using laser-produced plasmas and grazing-incidence spectrographs. The measured wavelengths are significant for the determination of quantum electrodynamics effects in highly charged ions. Ralchenko *et al.*[18] and Radtke *et al.*[19] identified E1 and magnetic dipole (M1) emission lines of Fe-like W ion using the Berlin EBIT. Their results indicated that some of the M1 lines are extremely useful towards the diagnosis of temperature and density of hot fusion devices. Louzon *et al.*[20] proposed the x-ray spectrum, in wavelengths ranging from 8 Å to 10 Å, and identified resonance transitions 3d–4f, 3d–5f, 3p–4d, and 3d–4p of Fe-like Sm ion employing laser-produced plasmas. Such measured wavelengths play a major role in testing the most advanced theories of relativistic atomic structure. The L-shell emission lines from Fe-like Au^{53+} ion are reported by Brown *et al.*[21] Its strong $3d_{5/2} \rightarrow 2p_{3/2}$ emission lines can be used for diagnosing charge state distribution in high energy density plasmas, for instance, those identified in the laser inlet hole of a hot cavity radiation source. With the aid of these experimental data, theoretical calculations not only enrich the family of HCIs, but also provide key insights into the identification of measured lines and explanation of the existing results. Guo *et al.*[5] predicted the energy levels, transition probabilities, and wavelengths of $3d^8$

[†] These authors contributed equally to this work.
[‡] Corresponding author. E-mail: gjiang@scu.edu.cn

© 2022 Chinese Physical Society and IOP Publishing Ltd

ground configurations in Fe-like Hf, Ta, W, and Au ions using the second-order relativistic many-body perturbation theory (RMBPT) and the parallel RCI methods. Taking advantage of the reliable Flexible Atomic Code (FAC) and MCDHF as well as multi-configuration Dirac–Fock (MCDF) methods, the theoretical group has filled a gap in excitation energies, oscillator strengths, wavelengths, line strengths, radiative lifetimes, transition rates of electric quadrupole (E2), and M1 transitions of the $3s^23p^63d^8$ ground configurations for Fe-like ions ($Z = 72$–83).[22–24]

Despite intensive experimental and theoretical efforts, there is still a lack of complete and unambiguous atomic data of lanthanide elements. The atomic data of lanthanide elements were expected in many high-tech fields, including lighting, optoelectronic applications, atomic clocks, and so on.[25] These absent lines of lanthanide elements in different ionization stages contribute crucially to detecting the growth of peculiar stars in astrophysics.[26] Moreover, lanthanides were used for studying the ejected materials of neutron star mergers, especially for addressing nucleosynthesis and star formation.[27] Of particular interest are some emission lines of La and Sm ions found in the spectra of solar flares and corona.[28] In addition, it should be stressed that integrated radiation data of highly charged Gd and Tb elements are needed for the next generation of EUV lithography as the origin of light sources.[29] Unfortunately, little has been decided about the available atomic data of lanthanide elements, in particular Fe-like ions ($Z = 57, 60, 62, 64, 65$), needed for laboratory and astrophysical plasmas modeling and diagnosing.

In this paper, we established a consistent set of energy levels, wavelengths, transition rates, oscillator strengths, and line strengths for the lowest 21 states of $3p^63d^8$–$3p^53d^9$ E1 transitions configurations in Fe-like ions ($Z = 57, 60, 62, 64, 65$) using the MCDHF method. The correlation effects of VV and CV electrons were systematically considered. Meanwhile, we employed Breit interaction and QED corrections to treat accurately atomic state wave functions. Our results are in excellent agreement with the previous observations, indicating that our theoretical calculations are reliable. Moreover, we predicted some new transition data, offering actionable insights for future experiments. The layout of this paper is as follows: In Section 2, we introduce the theoretical methods and calculational details. In Section 3, we present the results and discussions of our calculated atomic parameters. We make a summary in Section 4.

2. Methods

2.1. MCDHF theory

In this paper, all of our calculations are carried out on basis of the MCDHF[30–32] approach, as implemented in GRASP2018 general relativistic atomic structure code. Some significant details have been extensively discussed elsewhere,[33–38] in which the Dirac–Coulomb Hamiltonian can be expressed as

$$H_{\mathrm{DC}} = \sum_{i=1}^{N} \left[c\boldsymbol{\alpha}_i \cdot \boldsymbol{p}_i + (\beta_i - 1)c^2 + V_i^N \right] + \sum_{i<j}^{N} \frac{1}{r_{ij}}, \tag{1}$$

where $\boldsymbol{\alpha}_i$ and β_i represent the 4×4 Dirac matrices, V_i^N represents the monopole part of the Coulomb interaction between electron–nucleus, and c represents the speed of light in atomic units. The atomic state functions (ASFs) constructed from linear combinations of symmetry adapted configuration state functions (CSFs) can be calculated through

$$\psi(\gamma PJM) = \sum_{i=1}^{N_{\mathrm{CSFs}}} c_i \Phi(\gamma_i PJM), \tag{2}$$

where P is the parity, J and M being, respectively, the total angular quantum number and the magnetic quantum number. N_{CSFs} is the number of CSFs and c_i denotes the configuration mixing coefficients for the state i. γ_i represents other appropriate labeling of the configuration state function i, *e.g.*, coupling scheme and orbital occupancy. The calculations on many levels are performed in the so-called extended optimal level (EOL) scheme. Under the relativistic self-consistent field (RSCF) procedure,[39] both the radial parts of the Dirac orbitals and expansion coefficients c_i are optimized to self-consistency.[39] In calculations based on the subsequent RCI, the Breit interaction

$$H_{\mathrm{Breit}} = -\sum_{i<j}^{N} \left[\boldsymbol{\alpha}_i \cdot \boldsymbol{\alpha}_j \frac{\cos(\omega_{ij} r_{ij}/c)}{r_{ij}} + (\boldsymbol{\alpha}_i \cdot \boldsymbol{\nabla}_i)(\boldsymbol{\alpha}_j \cdot \boldsymbol{\nabla}_j) \frac{\cos(\omega_{ij} r_{ij}/c) - 1}{\omega_{ij}^2 r_{ij}/c^2} \right], \tag{3}$$

and leading QED corrections (self-energy and vacuum polarization) have also been taken into consideration.[40,41]

The ASFs are established by the expansions of the *jj*-coupled CSFs.[42] To match the label of calculated states with that of the reference values, the *jj*-coupled CSFs were transformed to *LSJ*-coupled CSFs using the jj2lsj program developed by Gaigalas *et al.*[43,44] For a set of wave functions possessing the same J and parity, the atomic state is given by the label of the CSFs with the largest expansion coefficient. For the fine-structure energy levels, the estimated uncertainty between computed energy levels and experimental values can be calculated by[45]

$$\delta E_x = |\Delta x - 1|, \tag{4}$$

where $\Delta x = E_x(\text{experiment})/E_x(\text{theory})$, $x = \text{fs}$ presents the fine structure of a given spectral term.

2.2. Transition parameters

The transition properties for multipole transitions of rank k from γPJM_J to $\gamma' P'J'M'_J$ can be expressed as[37]

$$\left\langle \Psi\left(\gamma PJM_J\right) \left\| Q_k^{(\lambda)} \right\| \Psi\left(\gamma' P'J'M'_J\right) \right\rangle, \tag{5}$$

where $Q_k^{(\lambda)}$ denotes multipole transition operator in Coulomb or Babushkin gauge. To compute the transition matric element of two atomic state functions described by different sets of orbitals, a biorthogonal transformation[46] was adopted. The evaluation of matrix elements is implemented with standard Racah algebra techniques.[46]

For electric multipole transitions, such as E1 and E2 transitions, there are two gauges, *i.e.*, the Coulomb and Babushkin gauges, corresponding to velocity and length forms of the non-relativistic case, respectively. In theory, if the exact wave function is used to calculate the transition parameters, the values obtained by the velocity form are equal to that of the length form. In self-consistent field calculations, the length form is generally preferred results, since it is more sensitive to the accuracy of the wave function when compared to the velocity results.[26] The uncertainty $\mathrm{d}T$ of the calculated transition rates is described as[47,48]

$$\mathrm{d}T = \frac{|A_l - A_v|}{\max\left(A_l, A_v\right)}, \tag{6}$$

where A_l and A_v are transition rates in length and velocity forms, respectively.

2.3. Calculational procedure

For Fe-like ions, in our calculations, $1s^2 2s^2 2p^6 3s^2$ is treated as the core electrons. The even and odd parities belonging to $3p^6 3d^8$ and $3p^5 3d^9$ configurations were calculated separately. CSFs are obtained by the active set approach,[49] by allowing single and double (SD) excitations from the $n = 3$ shells of reference configurations to active set of orbitals with $n \leq 7$, $l \leq 4$, in which only one electron substitutions are allowed from the 3s core-shell. No substitutions are allowed from the $n = 1, 2$ shells, which is defined as an inactive closed core. VV and CV electron correlation effects are generally considered in this way. Taking into account the lists of CSFs increase very rapidly with the expanding active set of orbitals, we only retain the CSFs that directly interact with it in the reference configurations.[22–40] To check the convergence of computed parameters, active orbitals are enlarged step by step in a systematic way. The optimization is also layer by layer. At each stage, the newly added orbitals are optimized, while the previous ones are fixed. After that, Breit interaction in the low-frequency limit and QED corrections (*e.g.*, self-energy and vacuum polarization) are included in the RCI calculations.

3. Results and discussion

3.1. Energy levels

We begin by monitoring the convergence of our MCDHF calculations. For Fe-like Sm^{36+} ion, the resulting energies of the lowest 21 states belonging to the $3p^6 3d^8$ and $3p^5 3d^9$ configurations with respect to increasing active set of orbitals are concluded in Table 1. Obviously, from Table 1 we can find the energy differences between adjacent n are decreased gradually upon increasing active set of orbitals n. For these energy levels, the mean relative differences are around 0.36%, 0.22%, 0.01%, and 0.01% for calculations based on the expansion from $n = 3$ and expansions obtained from SD excitations to active sets $n = 4$, 5, 6, and 7. The calculated energy levels of all states at $n = 7$ active orbital are almost the same as those of all states at $n = 6$ active orbital. The maximum difference between $n = 7$ and $n = 6$ calculations is even less than 132 cm^{-1}. Such facts indicate the energy levels have converged when the active set of orbitals n is increased to 7. Subsequently, the same computational scheme then proceeded to monitor the convergence of other Fe-like ions ($Z = 57$, 60, 64, 65). Similar to Fe-like Sm^{36+} ion, we concluded that these selected ions possess identical trends of variation in energy upon increasing active set of orbitals. Excitation energies were predicted to converge successfully with active set of orbitals n increased to 7. At $n = 7$, the identified maximum differences are 152 cm^{-1}, 138 cm^{-1}, 127 cm^{-1}, and 77 cm^{-1} for Fe-like ions ($Z = 57$, 60, 64, 65) relative to $n = 6$ calculations, respectively. The computed energy levels with $n = 7$ are presented in Table S1 of supporting information for all Fe-like ions ($Z = 57$, 60, 62, 64, 65).

For comparison, the experimental values by Ekberg *et al.*[16] using laser-produced plasmas and the energy differences between theoretical and experimental results are summarized together in Table S1 of supporting information. From the inspection of Table S1, it should be pointed out that our simulated energy levels, aside from four levels ($3p^6 3d^8\ ^3P_0$, $3p^5 3d^9\ ^3P_0$, $3p^5 3d^9\ ^3F_2$, and $3p^5 3d^9\ ^1P_1$), agree fairly well with experimental results for Fe-like Sm^{36+} ion, with the difference less than 1000 cm^{-1}. The energy level of $3p^5 3d^9\ ^3F_2$ state is determined to be 3769876 cm^{-1}, which deviates from experimental value (3771340 cm^{-1}) up to 1464 cm^{-1}, the reason behind this is that the CV correlation effect arising from subshell 2p is not included in our calculation. Prior literature has found that these facts have a significant impact on energy levels.[50,51] Herein, since the limitation of available computational resources, the electron correlation effects are not fully considered. In fact, the atomic parameters of Fe-like Sm^{36+} ion have been investigated by Ivanova *et al.*[52] by means of the relativistic perturbation theory method of the zero-approximation model. For reference, their computed data

together with energy differences compared to available data reported by Ekberg *et al.*[16] are summarized in Table S1 of supporting information. It is apparent that most of the energy levels deviate from the experimental values significantly. For example, we note that the energy levels of $3p^63d^8\ ^3P_0$, $3p^53d^9\ ^3P_0$, $3p^53d^9\ ^3P_2$, $3p^53d^9\ ^1F_3$, and $3p^53d^9\ ^3F_2$ states are reported to be 162800 cm^{-1}, 2829200 cm^{-1}, 3634600 cm^{-1}, 3695800 cm^{-1}, 3763600 cm^{-1}, respectively. These results are far away from experimental values up to 6210 cm^{-1}, 6290 cm^{-1}, 7630 cm^{-1}, 8790 cm^{-1}, and 7740 cm^{-1}. Compared with the relativistic perturbation theory method of the zero-approximation model, we concluded that MCDHF calculations with the inclusion of electron correlation effects and higher-order corrections are more suitable to investigate atomic parameters of Fe-like ions. Subsequently, we proceed to investigate energy levels of other Fe-like ions ($Z = 57$, 60, 64, 65) using MCDHF method, the obtained results are listed in Table S1 of supporting information. Meanwhile, in the last column of Table S1, we list the estimated uncertainty $\delta E_{\rm fs}$ between the present energy levels and experiment values. Our results for energy levels of these Fe-like ions are in good agreement with observed ones by Ekberg *et al.*[16] The relative deviations are within 0.1% except for a few states, of which the largest relative difference is about 0.8% for the $3p^63d^8\ ^3P_0$ state. We expect that the current results can be used as a reference for other calculations of Fe-like sequence ions.

Table 1. Energy levels (all in unit cm^{-1}) for the lowest 21 states in Fe-like Sm^{36+} ion as a function of increasing active sets of orbitals.

Key	Configuration	$n = 3$	$n = 4$	$n = 5$	$n = 6$	$n = 7$
1	$3p^63d^8\ ^3F_4$					
2	$3p^63d^8\ ^1D_2$	62215.16	57540.55	56739.64	56692.05	56665.67
3	$3p^63d^8\ ^3P$	181491.12	172211.48	170587.22	170452.22	170386.93
4	$3p^63d^8\ ^3F_3$	212664.39	212750.24	212929.82	212959.82	212971.79
5	$3p^63d^8\ ^3P_2$	273398.11	270603.42	269626.59	269625.51	269609.88
6	$3p^63d^8\ ^3P_1$	307959.24	303906.98	301940.78	301924.28	301888.31
7	$3p^63d^8\ ^1G_4$	313542.40	311946.12	310595.30	310531.41	310494.95
8	$3p^63d^8\ ^3F_2$	473287.90	470400.24	470292.28	470303.73	470307.30
9	$3p^63d^8\ ^1S$	643672.88	631946.22	630533.17	630351.54	630278.01
10	$3p^53d^9\ ^3F_4$	2496588.81	2487823.28	2486602.43	2486438.43	2486422.45
11	$3p^53d^9\ ^1D_2$	2558483.83	2540452.86	2539261.11	2539057.43	2539016.67
12	$3p^53d^9\ ^3D_3$	2654285.46	2629387.48	2628287.16	2627977.39	2627908.73
13	$3p^53d^9\ ^3P_1$	2736559.06	2708719.67	2706194.12	2705843.88	2705745.17
14	$3p^53d^9\ ^3D_2$	2817329.69	2794892.76	2793701.44	2793452.13	2793400.47
15	$3p^53d^9\ ^3P$	2859570.55	2837245.44	2834446.47	2834203.21	2834129.16
16	$3p^53d^9\ ^3D_1$	2876458.51	2855317.33	2853621.48	2853312.16	2853234.59
17	$3p^53d^9\ ^3F_3$	2882767.75	2857566.96	2855663.65	2855369.47	2855304.28
18	$3p^53d^9\ ^3P_2$	3671089.61	3645285.69	3643198.30	3642889.53	3642776.16
19	$3p^53d^9\ ^1F_3$	3734472.77	3708328.33	3706107.86	3705705.01	3705574.08
20	$3p^53d^9\ ^3F_2$	3783899.82	3771359.70	3770085.17	3769921.86	3769876.36
21	$3p^53d^9\ ^1P_1$	3999426.52	3965179.42	3963295.55	3962903.79	3962772.22

Figure 1 shows the contribution of Breit interaction and QED corrections to the excitation energies for the lowest 21 states of $3p^63d^8$ and $3p^53d^9$ configurations in Fe-like Sm^{36+} ion. As displayed in Fig. 1, the total (Breit and QED) corrections reduce excitation energies by about 0.16%–2.09% and narrow the gap between the theoretical values and experimental observations, especially for the $3p^53d^9\ ^3F_2$ state, in which the energy is significantly decreased by around 30000 cm^{-1}. By contrast, the $3p^63d^8\ ^1D_2$ and $3p^63d^8\ ^3P_0$ states have somewhat higher energies than Coulomb energies by about 3000 cm^{-1} and 5000 cm^{-1}, respectively. And the accuracy of energies improved by about 5.48% and 3.20%. Overall, the improved agreement between the theoretical and experimental results suggests it is highly necessary to incorporate Breit and QED corrections for RCI calculations of the highly charged heavy ions.[53] Subsequently, we identify respectively the influence of Breit interaction and QED corrections on energy levels. The Breit correction reduce all energy levels (relative to Coulomb energies) of the $3p^63d^8$ and $3p^53d^9$ configurations by about 0.29%–2.21% (Fig. 1), with two exceptions: $3p^63d^8\ ^1D_2$ and $3p^63d^8\ ^3P_0$, respectively, in which the energies are higher than Coulomb energies by around 5.50% and 3.19% (Fig. 1). It should be stressed that the QED corrections have little effect on energy levels, the contribution to the energy levels appears in the range of around 0.01%–0.18%. We, therefore, concluded that Breit interaction is the dominant contribution to energy in the higher-order corrections.

Figures 2 and 3 present the effects of Breit interaction and QED corrections on energy levels of $3p^63d^8$ and $3p^53d^9$ configurations along the sequence, respectively. In Fig. 2, note that there are identical variation tendencies for levels 4 and 5, levels 7 and 9, levels 10 to 13, levels 14 to 17, thus we only present levels 2 to 4, levels 6 to 8, level 10, level 14, levels 18

to 21. It is shown from Fig. 2 that the contribution of Breit interaction is improved for each level considered with the nuclear charge Z increasing. The reason behind this is that the attraction between the nucleus and the extranuclear electrons is positively correlated with the nuclear charge Z. It is well known that Breit interaction is the embodiment of the interaction between electrons,[54] the Breit interaction thus enhance accordingly. Figure 3 shows the effect of the QED corrections on energy levels with respect to Z. Similarly, we only show levels 2 to 4, level 8, level 10, level 14, levels 18 and 20. Notably, these levels have the consistent tends for levels 4–7, levels 8 and 9, levels 10–13, levels 14–17, levels 18 and 19, levels 20 and 21, thus the latter is ruled out here. From Fig. 3 we found that the contribution of QED effects, as expected, increase with the increase of Z for a majority of the levels, this is because the QED corrections are proportional to Z^4. While for levels 3 and 20, the increasing Z leads to a reduction of the QED contribution, which is consistent with the conclusion summarized by Malyshev *et al.*[55] and Hu *et al.*[56]

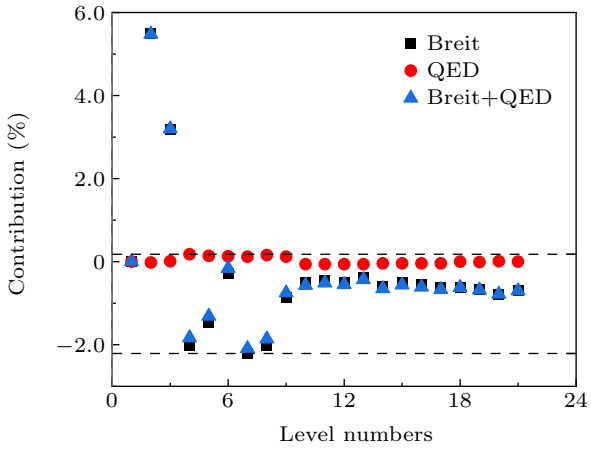


Fig. 1. Corrections of Breit and QED effects to the MCDHF energies for the lowest 21 states of $3p^63d^8$ and $3p^53d^9$ configurations in Fe-like Sm^{36+} ion, all energies are relative to the ground state.

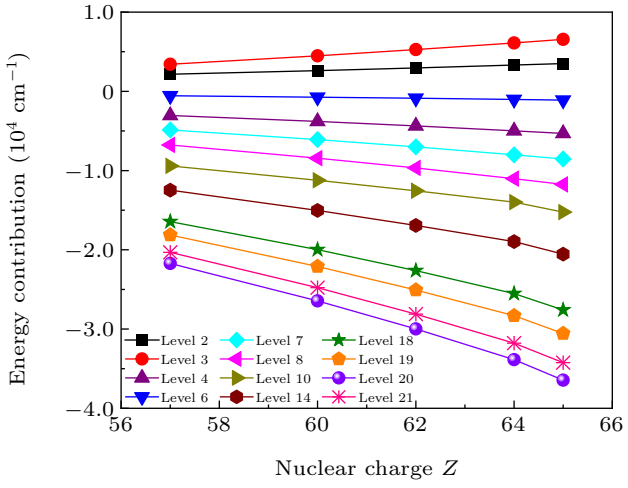


Fig. 2. Contribution from Breit interaction to the energy levels of $3p^63d^8$ and $3p^53d^9$ configurations for Fe-like ion as a function of nuclear charge Z.

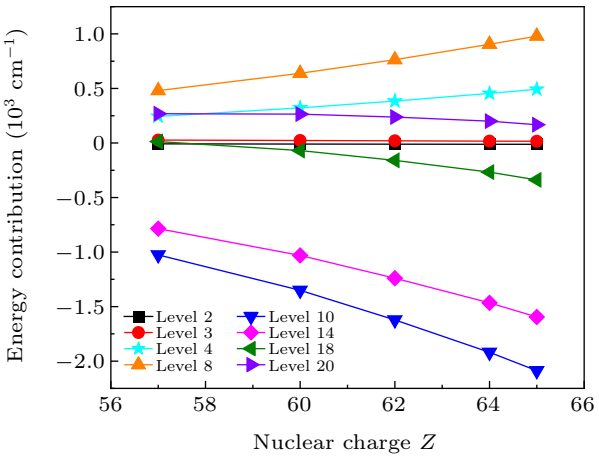


Fig. 3. Contribution from QED corrections to the energy levels of $3p^63d^8$ and $3p^53d^9$ configurations for Fe-like ion as a function of nuclear charge Z.

3.2. Transition parameters

Having decided the energy levels of all Fe-like ions (Z = 57, 60, 62, 64, 65), we further investigated the wavelengths λ, transition rates A, weighted oscillator strengths gf, line strengths S, and uncertainty estimators dT of $3p^63d^8$–$3p^53d^9$ E1 transitions configurations using MCDHF method. The resulting data are listed in Tables S2–S6 of supporting information. The E1 transition rates are given in both velocity (v) and length (l) forms. Our MCDHF transition rates in velocity forms (A_v) and length forms (A_l) show good agreement for strong transitions. Such results can be used as an indicator to verify the reliability of our calculations.[57] It should be noted that, however, there are substantial discrepancies between A_v and A_l for some weak transitions, this may be attributed to a small imbalance arising from correlation effects that alter the transition rates significantly in one of the gauges.[58] The other transition parameters, including weighted oscillator strengths gf and line strengths S, are presented with the length form, there is a widespread consensus which is generally thought to be more accurate than the velocity form.[59,60]

In Table 2, we have compared the E1 transitions wavelengths of Fe-like La^{31+}, Nd^{34+}, Sm^{36+}, and Gd^{38+} ions with the available experimental values. Interestingly, it is apparent from Table 2 that our E1 transitions wavelengths are overall consistent with the available experimental values reported by Ekberg *et al.*[16] again validating our calculation scheme. As shown in Table 2, for Fe-like Sm^{36+} ion, in most cases, our MCDHF wavelengths are shorter than the observations. Comparing our calculated and experimental values, the striking difference has been predicted to occur in the $3p^63d^8\ ^1G_4 \rightarrow 3p^53d^9\ ^1F_3$ transition level, whose value is −0.017 Å (relative difference of 0.058%), which is quite satisfactory. Regarding Fe-like La^{31+}, Nd^{34+}, and Gd^{38+} ions, the greatest deviation between our MCDHF values and experimental ones is found to be 0.041 Å, and the relative deviation of about 0.13%. Thus, we can conclude with confidence that our computed wavelengths are highly accurate, which is enough to determine

ground state correlation effects and quantum electrodynamics effects in highly charged ions.

Table 2. Comparison of wavelengths (in unit Å) for E1 transitions with the experimental values in Fe-like La^{31+}, Nd^{34+}, Sm^{36+}, and Gd^{38+} ions.

Lower level	Upper level	La^{31+}		Nd^{34+}	
		λ_{MCDHF}	Exp[16]	λ_{MCDHF}	Exp[16]
$3p^63d^8\ ^3P_1$	$3p^53d^9\ ^3D_1$				
$3p^63d^8\ ^3P_1$	$3p^53d^9\ ^3P_2$	36.74	36.750	32.48	32.500
$3p^63d^8\ ^1D_2$	$3p^53d^9\ ^3P_1$	43.74	43.758	39.99	40.005
$3p^63d^8\ ^3P_2$	$3p^53d^9\ ^3D_1$	44.63	44.671	40.94	40.964
$3p^63d^8\ ^3F_2$	$3p^53d^9\ ^1P_1$	35.01	35.046	31.02	31.030
$3p^63d^8\ ^1D_2$	$3p^53d^9\ ^1D_2$	46.68	46.690	42.68	42.686
$3p^63d^8\ ^3P_2$	$3p^53d^9\ ^3D_2$			41.94	41.941
$3p^63d^8\ ^3P_2$	$3p^53d^9\ ^3P_2$	36.35	36.369	32.16	32.176
$3p^63d^8\ ^3F_2$	$3p^53d^9\ ^3F_2$			32.91	32.916
$3p^63d^8\ ^1D_2$	$3p^53d^9\ ^3D_3$				
$3p^63d^8\ ^3P_2$	$3p^53d^9\ ^1F_3$	35.51	35.551		
$3p^63d^8\ ^3F_3$	$3p^53d^9\ ^3D_2$	44.78	44.804	41.02	41.028
$3p^63d^8\ ^3F_3$	$3p^53d^9\ ^3P_2$	35.72	35.746	31.61	31.633
$3p^63d^8\ ^3F_3$	$3p^53d^9\ ^3F_3$	43.72	43.758	40.05	40.071
$3p^63d^8\ ^3F_3$	$3p^53d^9\ ^1F_3$	34.91	34.947	30.99	31.030
$3p^63d^8\ ^3F_4$	$3p^53d^9\ ^3D_3$	44.12	44.139	40.32	40.336
$3p^63d^8\ ^3F_4$	$3p^53d^9\ ^3F_3$				
$3p^63d^8\ ^1G_4$	$3p^53d^9\ ^3F_3$	45.47	45.506	41.61	41.627
$3p^63d^8\ ^1G_4$	$3p^53d^9\ ^1F_3$	36.02	36.051	31.92	31.946
$3p^63d^8\ ^3F_4$	$3p^53d^9\ ^3F_4$	46.55	46.557	42.60	42.595
Lower level	Upper level	Sm^{36+}		Gd^{38+}	
		λ_{MCDHF}	Exp[16]	λ_{MCDHF}	Exp[16]
$3p^63d^8\ ^3P_1$	$3p^53d^9\ ^3D_1$	39.19	39.200		
$3p^63d^8\ ^3P_1$	$3p^53d^9\ ^3P_2$	29.93	29.941		
$3p^63d^8\ ^1D_2$	$3p^53d^9\ ^3P_1$	37.75	37.760		
$3p^63d^8\ ^3P_2$	$3p^53d^9\ ^3D_1$	38.71	38.720	36.63	36.643
$3p^63d^8\ ^3F_2$	$3p^53d^9\ ^1P_1$	28.63	28.646	26.43	26.461
$3p^63d^8\ ^1D_2$	$3p^53d^9\ ^1D_2$	40.28	40.285	38.07	38.060
$3p^63d^8\ ^3P_2$	$3p^53d^9\ ^3D_2$	39.62	39.618		
$3p^63d^8\ ^3P_2$	$3p^53d^9\ ^3P_2$	29.65	29.651	27.34	27.352
$3p^63d^8\ ^3F_2$	$3p^53d^9\ ^3F_2$	30.31	30.302		
$3p^63d^8\ ^1D_2$	$3p^53d^9\ ^3D_3$	38.89	38.896		
$3p^63d^8\ ^3P_2$	$3p^53d^9\ ^1F_3$	29.10	29.115		
$3p^63d^8\ ^3F_3$	$3p^53d^9\ ^3D_2$	38.75	38.754	36.66	36.643
$3p^63d^8\ ^3F_3$	$3p^53d^9\ ^3P_2$	29.16	29.160		
$3p^63d^8\ ^3F_3$	$3p^53d^9\ ^3F_3$	37.85	37.858		
$3p^63d^8\ ^3F_3$	$3p^53d^9\ ^1F_3$	28.63	28.646	26.45	26.461
$3p^63d^8\ ^3F_4$	$3p^53d^9\ ^3D_3$	38.05	38.058	35.96	35.978
$3p^63d^8\ ^3F_4$	$3p^53d^9\ ^3F_3$	35.02	35.022		
$3p^63d^8\ ^1G_4$	$3p^53d^9\ ^3F_3$	39.30	39.298	37.15	37.147
$3p^63d^8\ ^1G_4$	$3p^53d^9\ ^1F_3$	29.45	29.467	27.18	27.197
$3p^63d^8\ ^3F_4$	$3p^53d^9\ ^3F_4$	40.22	40.206	38.02	38.007

Finally, we estimate uncertainty dT on the transition rate A (in unit s^{-1}) for Fe-like Sm^{36+} ion. It is widely accepted for evaluating the quality of E1 transition rates. The smaller the uncertainty dT, the higher quality of E1 transition rates. As shown in Fig. 4, the uncertainty dT agrees within 10% for most of the strong transitions. Moreover, for the strong lines observed from $3p^63d^8\ ^3P_1 \rightarrow 3p^53d^9\ ^3D_1$ together with $3p^63d^8\ ^3P_2 \rightarrow 3p^53d^9\ ^3D_2$ transitions, the uncertainty dT is well below 0.1%. In contrast to these stronger transitions, the uncertainty dT is relatively larger for the small amounts of weaker transitions. This situation is reasonable and has a precedent, where the authors found that some weaker transitions are composed of two-electron or intercombination lines transitions, the transition rates for this kind of transition are difficult to compute accurately.[61,62]

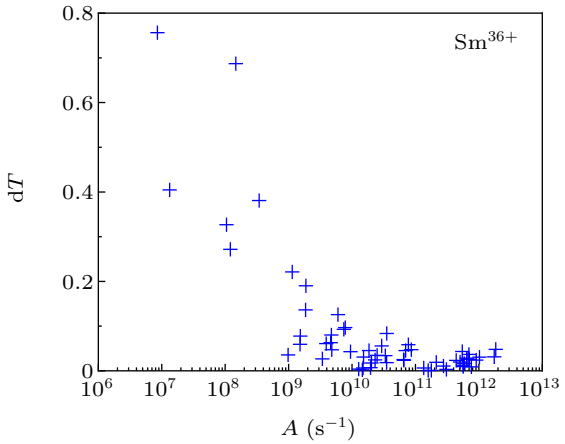


Fig. 4. The uncertainty estimators dT for transition rates A (in unit s^{-1}) of E1 transitions in Fe-like Sm^{36+} ion.

4. Conclusions

Using the MCDHF method, we have performed a comprehensive investigation on the energy levels among the lowest 21 states of the $3p^63d^8$ and $3p^53d^9$ configurations in Fe-like ions ($Z = 57$, 60, 62, 64, 65). Our results of energy levels are in good agreement with available experimental measurements. The relative differences agree with within 0.1% for a majority of the energy levels. Our detailed discussion suggests that it is highly necessary to consider electron correlation effects and higher-order corrections in calculations of the highly charged heavy ions. For transition data, we have reported the transition wavelengths. Compared with the experimental data, the overall deviation is well below 0.041 Å. The uncertainty dT of transition rate A (in unit s^{-1}) agree to within 10% for most of the strong E1 transitions. Overall, our calculations indicated that the MCDHF method with the inclusion of more electron correlation effects and higher-order corrections is more accurate than the relativistic perturbation theory approach towards identifying atomic data of Fe-like ions. Additionally, we have obtained a new set of transition parameters, namely, wavelengths, transition rates, weighted oscillator strengths, and line strengths for E1 transitions. These results would benefit lines identification, modeling of astrophysical and laboratory plasmas.

Acknowledgment

The authors express sincere appreciation to professor Jönsson P for providing the GRASP2018 program for free.

References

[1] Guo X L, Huang M, Yan J, Li S, Wang K, Si R and Chen C Y 2015 *Chin. Phys. B* **25** 013101
[2] Fan J Z, Zhang D H, Chang Z W, Shi Y L and Dong C Z 2012 *Chin. Phys. Lett.* **29** 073102
[3] Liu J P, Li C B and Zou H X 2017 *Chin. Phys. B* **26** 103201
[4] Aggarwal S, Singh J and Mohan M 2013 *Chin. Phys. B* **22** 033201
[5] Guo X L, Huang M, Yan J, Li S, Si R, Li C Y, Chen C Y, Wang Y S and Zou Y M 2015 *J. Phys. B: At. Mol. Opt. Phys.* **48** 144020
[6] Wu T, Kawasaki H, Shimada Y, Higashiguchi T and O'Sullivan G 2020 *J. Phys. B: At. Mol. Opt. Phys.* **53** 225701
[7] Aggarwal S, Jha A K S, Khatri I, Singh N and Mohan M 2015 *Chin. Phys. B* **24** 053201
[8] Silwal R, Dreiling J M, Sanders S C, Takacs E and Ralchenko Y 2020 *J. Phys. B: At. Mol. Opt. Phys.* **53** 145002
[9] Sheil J, Dunne P, Higashiguchi T, Kos D, Long E, Miyazaki T, O'Reilly F, O'Sullivan G, Sheridan P and Suzuki C 2017 *J. Phys. B: At. Mol. Opt. Phys.* **50** 065006
[10] Aggarwal S 2014 *Chin. Phys. B* **23** 093203
[11] Wu T, Higashiguchi T, Li B, Arai G, Hara H, Kondo Y, Miyazaki T, Dinh T H, Dunne P, O'Reilly F and Sokell E 2016 *J. Phys. B: At. Mol. Opt. Phys.* **49** 035001
[12] Shang X, Tian Y, Wang Q, Fan S, Bai W and Dai Z 2014 *Mon. Not. R. Astron. Soc.* **442** 138
[13] Shang X, Wang Q, Tian Y, Wang C and Dai Z 2015 *J. Phys. B: At. Mol. Opt. Phys.* **48** 085001
[14] Doron R, Fraenkel M, Mandelbaum P, Zigler A and Schwob J L 1998 *Phys. Scr.* **58** 19
[15] Witthoeft M C, Bautista M A, Garcia J, Kallman T R, Mendoza C, Palmeri P and Quinet P 2011 *Astrophys. J. Suppl. Ser.* **196** 7
[16] Ekberg J O, Feldman U and Reader J 1988 *J. Opt. Soc. Am. B* **5** 1275
[17] Ekberg J O, Seely J F, Feldman U, Brown C M and Hulburt E O 1989 *J. Opt. Soc. Am. B* **6** 1648
[18] Ralchenko Y, Draganic I N, Osin D, Gillaspy J D and Reader J 2011 *Phys. Rev. A* **83** 032517
[19] Radtke R, Biedermann C, Mandelbaum P and Schwob J L 2007 *J. Phys. Conf. Ser.* **58** 113
[20] Louzon E, Henis Z, Levi I, Hurvitz G, Ehrlich Y, Fraenkel M, Maman S and Mandelbaum P 2009 *J. Opt. Soc. Am. B* **26** 959
[21] Brown G V, Hansen S B, Träbert E, Beiersdorfer P, Widmann K, Chen H, Chung H K, Clementson J H T and Gu M F 2008 *Phys. Rev. E* **77** 066406
[22] Zhao Z L, Wang K, Li S, Si R, Chen C Y, Chen Z B, Yan J and Ralchenko Y 2018 *At. Data Nucl. Data Tables* **119** 314
[23] Quinet P 2011 *J. Phys. B: At. Mol. Opt. Phys.* **44** 195007
[24] Clementson J, Beiersdorfer P, Brage T and Gu M F 2014 *At. Data Nucl. Data Tables* **100** 577
[25] Wang K, Zhang C Y, Si R, Li S, Chen Z B, Zhao X H, Chen C Y and Yan J 2018 *At. Data Nucl. Data Tables* **123–124** 114
[26] Chen Z B, Ma K, Wang H J, Wang K, Liu X B and Zeng J L 2017 *At. Data Nucl. Data Tables* **113** 258
[27] Radžiūtė L, Gaigalas G, Kato D, Rynkun P and Tanaka M 2020 *Astrophys. J. Suppl. Ser.* **248** 17
[28] Goyal A, Khatri I, Aggarwal S, Singh A K and Mohan M 2016 *At. Data Nucl. Data Tables* **107** 406
[29] Podpaly Y A, Gillaspy J D, Reader J and Ralchenko Y 2014 *J. Phys. B: At. Mol. Opt. Phys.* **48** 025002
[30] Li X F and Jiang G 2018 *Chin. Phys. B* **27** 073101
[31] Grant I P 2007 *Relativistic Quantum Theory of Atoms and Molecules*, Vol. 40 (New York: Springer) p. 384
[32] He X K, Liu J P, Zhang X, Shen Y and Zou H X 2018 *Chin. Phys. B* **27** 083102
[33] Hao L H and Kang X P 2014 *Eur. Phys. J. D* **68** 1
[34] Hu F 2021 *Radiat. Phys. Chem.* **108** 109293
[35] Hao L H, Jiang G, Song S and Hu F 2008 *At. Data Nucl. Data Tables* **94** 739
[36] Fischer C F, Godefroid M, Brage T, Jönsson P and Gaigalas G 2016 *J. Phys. B: At. Mol. Opt. Phys.* **49** 182004
[37] Jönsson P, He X, Fischer C F and Grant I P 2007 *Comput. Phys. Commun.* **177** 597
[38] Li X F, Jia L P, Wang H B and Jiang G 2021 *Chin. Phys. B* **30** 053102
[39] Jönsson P, Gaigalas G, Bieroń J, Fischer C F and Grant I P 2013 *Comput. Phys. Commun.* **184** 2197
[40] Fischer C F, Gaigalas G, Jönsson P and Bieroń J 2019 *Comput. Phys. Commun.* **237** 184
[41] Grant I P, McKenzie B J, Norrington P H, Mayers D F and Pyper N C 1980 *Comput. Phys. Commun.* **21** 207
[42] Sturesson L, Jönsson P and Fischer C F 2007 *Comput. Phys. Commun.* **177** 539
[43] Gaigalas G, Žalandauskas T and Rudzikas Z 2003 *At. Data Nucl. Data Tables* **84** 99
[44] Gaigalas G, Fischer C F, Rynkun P and Jönsson P 2017 *Atoms* **5** 6
[45] Hao L H, Jiang G and Hou H J 2010 *Phys. Rev. A* **81** 022502
[46] Olsen J, Godefroid M R, Jönsson P, Malmqvist P Å and Fischer C F 1995 *Phys. Rev. E* **52** 4499
[47] Fischer C F 2009 *Phys. Scr.* **T134** 014019
[48] Ekman J, Godefroid M R and Hartman H 2014 *Atoms* **2** 215
[49] Hao L, Jiang G, Hu F, Wang C K, Wang Z B and Yang J M 2013 *Chin. Phys. B* **22** 073202
[50] Hu F, Sun Y, Mei M, Pan Y, Wu M and Liu H 2021 *J. Quantum Spectrosc. Radiat. Transfer* **273** 107842
[51] Hao L H and Jiang G 2011 *Phys. Rev. A* **83** 012511
[52] Ivanova E P and Tsirekidze M A 1986 *Phys. Scr.* **34** 35
[53] Khatri I, Goyal A, Aggarwal S, Singh A K and Mohan M 2015 *Chin. Phys. B* **24** 103202
[54] Wang H W, Zhang L, Jiang G, Li X F and Wang H B 2018 *Indian J. Phys.* **92** 137
[55] Malyshev A V, Glazov D A, Kozhedub Y S, Anisimova I S, Kaygorodov M Y, Shabaev V M and Tupitsyn I I 2021 *Phys. Rev. Lett.* **126** 183001
[56] Hu F, Yang J, Wang C, Jing L, Chen S, Jiang G and Hao L 2011 *Phys. Rev. A* **84** 042506
[57] Sun L, Wu M and Jiang G 2019 *Indian J. Phys.* **94** 1
[58] Jönsson P and Bieroń J 2010 *J. Phys. B: At. Mol. Opt. Phys.* **43** 074023
[59] Wang K, Chen Z B, Zhao X H, Chen C Y and Yan J 2019 *J. Quantum Spectrosc. Radiat. Transfer* **237** 106640
[60] Wang K, Zhang X H, Zhang C Y, Dang W, Zhao X H, Chen Z B, Si R, Chen C Y and Yan J 2021 *J. Quantum Spectrosc. Radiat. Transfer* **261** 107512
[61] Atalay B, Brage T, Jönsson P and Hartman H 2019 *Astron. Astrophys.* **631** A29
[62] Li W, Hartman H, Wang K and Jönsson P 2020 *Astron. Astrophys.* **643** A156